2186 *Biochemistry* **2010,** *49,* 2186–2193
DOI: 10.1021/bi902176v

BIOCHEMISTRY
including biophysical chemistry & molecular biology
Article

Solution Structure of an Acyl Carrier Protein Domain from a Fungal Type I Polyketide Synthase[†,‡]

Pakorn Wattana-amorn, Christopher Williams, Eliza Płoskoń, Russell J. Cox, Thomas J. Simpson, John Crosby, and Matthew P. Crump*

School of Chemistry, University of Bristol, Cantock's Close, Bristol BS8 1TS, U.K.

Received December 18, 2009; Revised Manuscript Received February 3, 2010

ABSTRACT: Acyl (peptidyl) carrier protein (ACP or PCP) is a crucial component involved in the transfer of thiol ester-bound intermediates during the biosynthesis of primary and secondary metabolites such as fatty acids, polyketides, and nonribosomal peptides. Although many carrier protein three-dimensional structures have been determined, to date there is no model available for a fungal type I polyketide synthase ACP. Here we report the solution structure of the norsolorinic acid synthase (NSAS) holo ACP domain that has been excised from the full-length multifunctional enzyme. NSAS ACP shows similarities in three-dimensional structure with other type I and type II ACPs, consisting of a four-helix bundle with helices I, II, and IV arranged in parallel. The N-terminus of helix III, however, is unusually hydrophobic, and Phe1768 and Leu1770 pack well with the core of the protein. The result is that unlike other carrier proteins, helix III lies almost perpendicular to the three major helices. Helix III is well-defined by numerous NMR-derived distance restraints and may be less flexible than counterparts in type II FAS and PKS ACPs. When the holo ACP is derivatized with a hexanoyl group, only minor changes are observed between the HSQC spectra of the two ACP species and no NOEs are observed for this hydrophobic acyl group. Along with the mammalian type I FAS, this further strengthens the view that type I ACPs do not show any significant affinity for hydrophobic (nonpolar) chain assembly intermediates attached via the 4′-phosphopantetheine prosthetic group.

Acyl carrier (ACP)[1] and their peptidyl carrier protein (PCP) analogues are key components of fatty acid (FAS), polyketide (PKS) synthases and nonribosomal peptide synthetases (NRPS), playing an essential role in the transfer of starter and extender units and acyl intermediates to the correct enzymatic partners during biosynthesis. This combined with their small size and stability has meant that the structures and acyl binding properties of ACPs from type I and type II FASs and PKSs have been the focus of studies by NMR and X-ray crystallography (*1*−*8*). Type II FAS ACP structures are particularly well studied, and comparisons of apo, holo, and acyl forms have revealed extensive conformational flexibility and the ability of these proteins to sequester bound acyl chains within an internal cavity (*4*, *8*−*10*). ACP structures and intermediate binding in polyketide synthases are less well studied than those features of their FAS counterparts, but the actinorhodin type II PKS ACP is known to show significant changes in conformation when it binds saturated carbon chains (*11*). Polar intermediates (which more closely resemble the assembly intermediates) exhibit only moderate affinity for the protein and may reside predominantly on the ketosynthase and chain length factor heterodimer during chain elongation (*12*). Fundamentally, however, the role of intermediate sequestration across type II systems is not well understood, and it may involve elements of protein recognition, stabilization, and protection from other reactive intermediates. These features, however, may not translate to type I synthases because the mammalian FAS ACP displays no binding of acyl side chains of different length fatty acids (*6*). This may be a facet of its integration into a larger covalently linked synthase where protection of chemically unstable intermediates by the ACP is not required and may be a function of the synthase as a whole.

To date, the ACP from module 2 of the 6-deoxyerythronolide B synthase (DEBS) from *Saccharopolyspora erythraea* is the only bacterial type I PKS ACP structure reported (*7*), and there are no examples of a fungal nonreducing type I PKS ACP. This is an important distinction as the type I modular ACP shuttles only a limited number of intermediates, whereas the iterative nonreducing ACP interacts with all of them. One of the best studied type I fungal systems is the norsolorinic acid synthase (NSAS). Norsolorinic acid is an intermediate in the biosynthesis of the carcinogen aflatoxin B_1, synthesized in the filamentous fungus *Aspergillus parasiticus* (*13*). NSAS is an iterative nonreducing PKS consisting of starter unit:ACP transacylase (SAT), ketosynthase (KS), malonyl-CoA:ACP transacylase (MAT), product template (PT), ACP, and thiolesterase/Claisen cyclase (TE/CLC)

[†]This work was supported by the Biotechnology and Biological Sciences Research Council (Grant BB/F014570/1 to P.W.-a.) and the Wellcome Trust (Grant WT082352MA to C.W.). We also thank the European Union for a studentship grant to E.P. under the Marie Curie Early Training Award scheme ('BRISENZ').

[‡]The ensemble of 20 NMR structures of holo ACP and associated NMR chemical shifts have been deposited in the Protein Data Bank and Biological Magnetic Resonance Data Bank as entries 2kr5 and 16624, respectively, for holo ACP.

*To whom correspondence should be addressed. Phone: +44 (0)117 3317163. Fax: +44 (0)117 9298611. E-mail: matt.crump@bristol.ac.uk.

[1]Abbreviations: FAS, fatty acid synthase; PKS, polyketide synthase; Act, actinorhodin; ACP, acyl carrier protein; NSAS, norsolorinic acid synthase; DEBS, 6-deoxyerythronolide B synthase; SAT, starter unit: ACP transacylase; KS, ketosynthase; MAT, malonyl-CoA:ACP transacylase; PT, product template; TE/CLC, thioesterase/Claisen cyclase; PCP, peptidyl carrier protein; T, thiolation domain; ESMS, electrospray mass spectrometry; rmsd, root-mean-square deviation; PKS^{ST}, sterigmatocystin polyketide synthase.

 Published on Web 02/05/2010

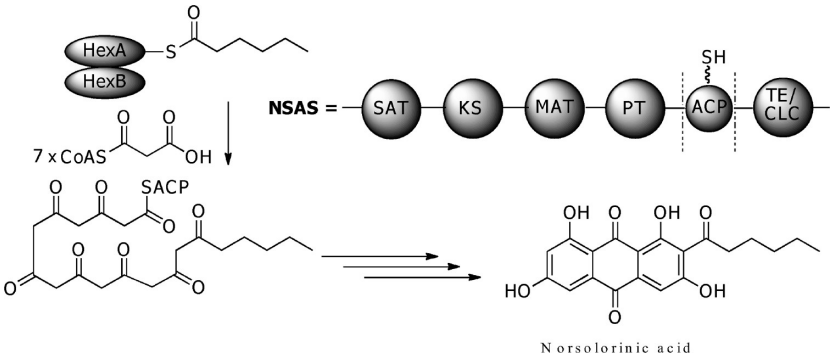

FIGURE 1: Biosynthetic pathway of norsolorinic acid.

domains (Figure 1). The biosynthesis of norsolorinic acid is initiated by condensation between a starter unit (hexanoyl-CoA) and an extender unit (malonyl-CoA). Hexanoyl-CoA is derived from a dedicated closely associated fatty acid synthase (HexA/HexB) and is selectively transferred to the PKS by the SAT domain (*14*). Extender units are loaded onto the ACP domain by the MAT (*15*), and successive Claisen condensations are catalyzed by the KS domain to generate an enzyme/ACP-bound octaketide. Formation of the first and second rings is controlled by the PT domain (*16*), followed by TE/CLC-catalyzed cyclization to form the third ring. All of these intermediate acyl species are shuttled between active sites via covalent attachment to the ACP domain.

Previously, we have shown that the excised ACP domain from NSAS can be modified by the *Streptomyces coelicolor* phosphopantetheinyl transferase (ACPS). The resulting NSAS holo ACP has the ability to replace the actinorhodin type II PKS ACP in vitro, in the presence of *S. coelicolor* malonyl transferase, producing two shunt products that have the same number of carbon atoms as actinorhodin itself (SEK4 and SEK4b) (*15*). However, any role that this type I PKS ACP may have in sequestration of the growing polyketide intermediate has yet to be determined. Here we report the first high-resolution structural information of a nonreducing fungal PKS ACP domain in the holo and acylated forms.

EXPERIMENTAL PROCEDURES

Preparation of ^{15}N- and ^{13}C-Enriched NSAS Apo, Holo, and Hexanoyl ACP Domains. The boundaries selected for the NSAS ACP were based on a sequence comparison with bacterial ACPs as described previously (*15*). The final construct contained residues 1705−1791 and was ligated into pET30b carrying a dual His_6 tag and S-tag fusion at the N-terminus. The NSAS ACP domain was expressed and purified as described previously (*15*). M9 minimal medium was used to prepare singly (^{15}N) and doubly (^{15}N and ^{13}C) enriched ACP with (^{15}N, 99%) NH_4Cl and (^{13}C, 98%) D-glucose (Cambridge Isotope Laboratories) as the sole nitrogen and carbon sources, respectively. Prior to NMR analysis, protein samples were incubated with recombinant enterokinase (Novagen) to cleave the N-terminal fusion tag. Two extra amino acids (**AM^{1705}**AKGVGV) remained at the N-terminus after removal of the tags. Enterokinase and the fusion tag were then removed by nickel affinity and gel filtration chromatography to yield NSAS apo ACP. NSAS apo ACP was incubated with CoA or hexanoyl-CoA substrate and *S. coelicolor* ACPS (*17*) to yield the holo or hexanoyl form, respectively. Complete conversion was confirmed by electrospray mass spectrometry (ESMS). Samples for NMR study were concentrated to 0.6−1.0 mM and buffer exchanged into 20 mM sodium acetate (pH 5.8) supplemented with 5 mM TCEP, 0.1 mM NaN_3, and a 5% D_2O/95% H_2O mixture. Phosphate buffer was used instead of sodium acetate in F_1- and F_2-filtered TOCSY, NOESY, and F_2-filtered NOESY experiments.

NMR Experiments for Structure Calculation. NMR data were recorded at 25 °C on a Varian INOVA spectrometer operating at 600 MHz. Standard triple-resonance experiments [HNCA, HN(CO)CA, HNCACB, CBCA(CO)NH, and HNCO] were conducted for the backbone assignment, and side chain assignments were obtained from C(CO)NH, HC(CO)NH, and HCCH-TOCSY experiments. Distance restraints were obtained from a simultaneous ^{15}N and ^{13}C NOESY-HSQC experiment (^{13}C/^{15}N NOESY) (150 ms mixing time). The unlabeled phosphopantetheine group was assigned using two-dimensional F_1- and F_2-filtered TOCSY and NOESY experiments, and protein−ligand interactions were identified using a two-dimensional F_2-filtered NOESY experiment (400 ms mixing time).

Structure Calculation. NMR data were processed using NMRPipe (*18*) and analyzed with CcpNmr Analysis version 1.0 (*19*). TALOS was used for the prediction of backbone ϕ and ψ torsion angles (*20*). Automated NOE assignment and structure calculation were performed using CNS and ARIA version 1.2 (*21*). The final ensemble of structures was further refined in explicit water using the RECOORD protocol (*22*).

RESULTS AND DISCUSSION

The NSAS Apo, Holo, and Hexanoyl-ACPs Adopt a Major and Minor Conformation. All uniformly ^{13}C and ^{15}N isotope-enriched NMR samples were purified to homogeneity by gel filtration chromatography. ESMS analysis confirmed the presence of a single mass for each ACP sample corresponding to 95−96% incorporation of ^{13}C and ^{15}N labels (calculated mass for the apo form of 9934 Da, observed mass of 9902 Da; calculated mass of the holo form of 10274 Da, observed mass of 10248 Da; calculated mass for hexanoyl-ACP of 10372 Da, observed mass of 10345 Da). The ^{1}H−^{15}N HSQC spectra of NSAS apo, holo, and hexanoyl-ACP, however, exhibited approximately 60% more than the predicted number of resonances [~96 signals expected (Figure 2)]. These extra peaks arise from a minor population that accounts for ~25% of the signal present. The same minor population was assigned in both the holo and hexanoyl-ACPs, and in each case, the residues were located at the N-terminus (residues 1707−1713) and in the loop between helices I and II (residues 1723−1741). This behavior is indicative

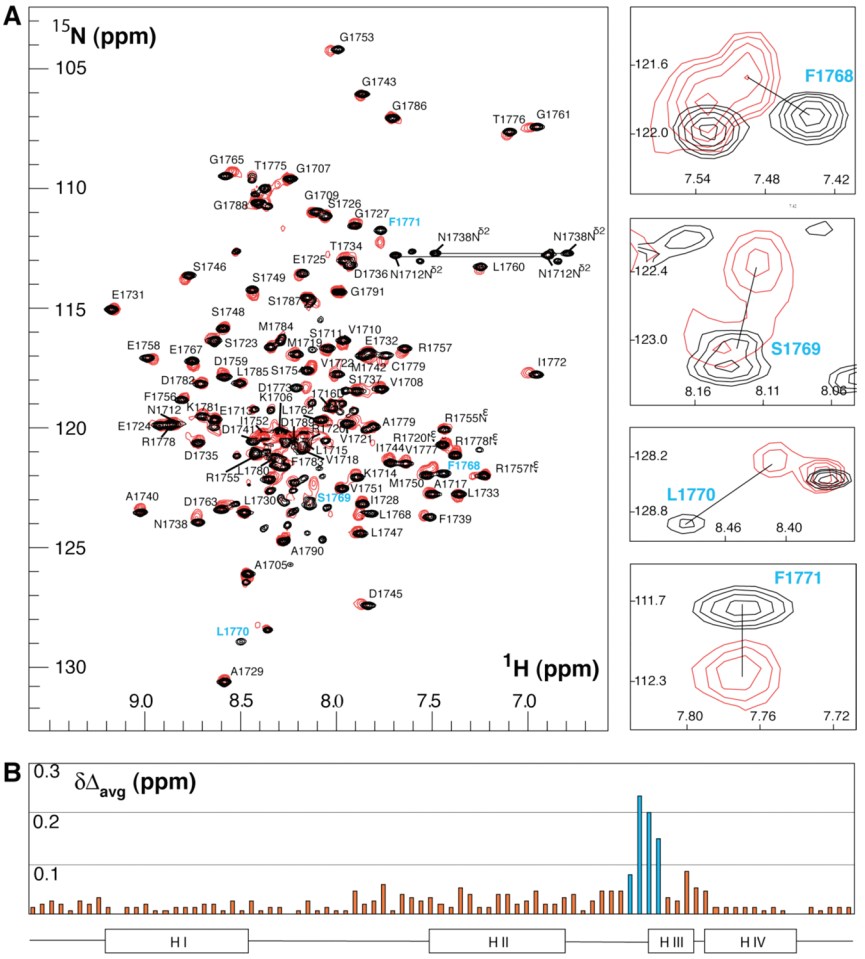

FIGURE 2: (A) Superimposed $^{1}H-^{15}N$ HSQC spectra of holo (black) and hexanoyl NSAS ACP (red) with expansions shown for Phe1768, Ser1769, Leu1770, and Phe1771 in helix III. (B) Chemical shift perturbation ($\delta\Delta_{avg}$) of the hexanoyl form compared to the holo form. Residues surrounding helix III with the most significant chemical shift changes are colored blue.

of the presence of at least two conformers in slow exchange with each other. A similar phenomenon has been observed for spinach apo and holo FAS ACP, although the exchange is quenched when the ACP is acylated and presumably stabilized (*4*). In addition, in the apo, holo, and hexanoyl NSAS ACP, several peaks remained unaccounted for and were too weak or ambiguous to be assigned, so the presence of further minor conformers cannot be ruled out. Multiple conformations have also been observed in the homologous peptidyl carrier protein (PCP) domain (also known as the thiolation domain), from tyrocidine NRPS (*23*), and such conformers may modulate interactions with partner enzymes. In the following section, we discuss the determination of the structure of the major conformation.

Structure of NSAS Holo ACP. All resonances were assigned from standard three-dimensional experiments, and NOE restraints for structure calculation were automatically assigned from a $^{13}C/^{15}N$ NOESY spectrum using ARIA (*21*). The final structures were calculated from 2869 NOE restraints and 58 torsion angle restraints. In the final calculations, 100 structures were generated and 20 of the lowest-energy structures were further water-refined (Figure 3). The quality of the structures was analyzed using WHATCHECK (*24*) and PROCHECK (*25*) (Table 1). The NSAS ACP domain consists of three major helices (helix I (residues 1712−1726), helix II (residues 1746−1760), and helix IV (residues 1776−1785) and a shorter third helix [helix III (residues 1770−1774)] lying perpendicular to helices II and IV (Figure 3). The N-terminus (residues 1705−1711) and the C-terminus (residues 1786−1791) are highly disordered and presumably form flexible linkers to neighboring domains in the full-length synthase. The core of NSAS ACP is formed from the hydrophobic packing of helical residues Val1708 and Val1722 (helix I), Ile1752 and Phe1756 (helix II), Leu1770 (helix III), and Leu1780 and Met1784 (helix IV) and the loop regions between helices I and II (Leu1733, Phe1739, and Ile1744) and helices II and III (Leu1762, Leu1764, and Phe1768). In type II FAS/PKS ACPs, helix III is generally six amino acids long and contains a greater proportion of both charged and less bulky amino acids. In NSAS ACP, however, these residues are replaced by the bulky hydrophobes Phe1768, Leu1770, and Phe1771 (Figure 4). Phe1768 packs tightly in the core of the structure rather than forming one of the polar faces of helix III, resulting in a less helical turn (Figure 4). Leu1770 is usually substituted with alanine in most other type II FAS/PKS ACPs. We also found that Phe1771 on helix III shows NOEs to Ser1746 and Ser1749 of helix II. This extensive hydrophobic packing makes helix III perpendicular to the other helices. We also observed weak NOE signals between the phosphopantetheine group and the side chain of L1747, indicating a weak interaction between the NSAS holo ACP and the phosphopantetheine arm as found in other holo ACPs (*5*, *26*).

Starter Unit-Bound NSAS Hexanoyl-ACP. Hexanoyl-ACP was prepared in vitro using *S. coelicolor* ACPS and hexanoyl-CoA to transfer the hexanoyl phosphopantetheinyl group onto apo ACP. The $^{1}H-^{15}N$ HSQC spectrum of

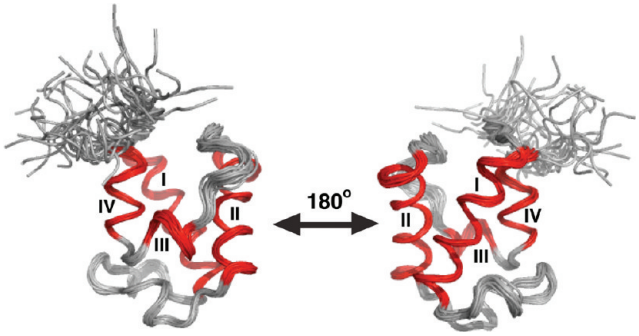

FIGURE 3: Final ensemble of NSAS holo ACP structures shown from two angles (without the phosphopantetheine cofactor).

Table 1: Structural Statistics and Quality Indicators for NSAS Holo ACP

	ensemble structure	lowest-energy structure
no. of NOE distance restraints		
unambigous	2136	
ambiguous	733	
intraresidue	969	
sequential	657	
short-range	463	
long-range	780	
dihedral angle (ϕ, ψ)	58	
energy (kcal/mol)		
E_{NOE}	165.1 ± 16.4	166.3
E_{DIHE}	488.8 ± 5.1	487.3
E_{VDW}	−718.0 ± 13.1	−711.6
E_{ELEC}	−3242.6 ± 64.2	−3359.1
no. of violations per structure		
NOE > 0.5 Å	0	0
TALOS > 5 Å	0	0
rmsd from restraints		
bonds (Å)	0.002 ± (< 0.001)	0.002
angles (deg)	0.375 ± 0.006	0.372
NOEs (Å)	0.024 ± 0.001	0.020
TALOS (deg)	0.31 ± 0.07	0.26
precision (rmsd to mean, Å)		
all residues (BB atom)	1.90 ± 0.44	2.60
well-ordered residues (BB atom)	0.35 ± 0.06	0.39
Ramachandran plot region (%)		
most favored	84.1	78.4
additionally allowed	14.7	21.6
generously allowed	0.5	0
disallowed	0.7	0
WHATCHECK Z score		
second-generation packing quality	−2.40	−2.36
Ramachandran plot appearance	−3.7	−4.0
χ_1/χ_2 rotamer normality	−2.8	−2.9
backbone conformation	−0.97	−0.65
no. of WHATCHECK		
bumps per 100 residues	5.8	5.6

hexanoyl-ACP revealed the changes to be localized to Phe1768, Ser1769, Leu1770, and Phe1771 that showed minor perturbations of 0.08−0.24 ppm when compared to the holo form (Figure 2). These residues precede or lie at the N-terminus of helix III, with Phe1768 and Leu1770 packing with the core of the structure. We have reported chemical shift perturbations in act ACP between the apo and holo ACP that could be attributed to an observable conformational change when high-resolution structures were determined (*26*). However, these changes were generally larger and more widely distributed than what we observe with NSAS ACP, with many residues in act ACP exhibiting differences of 0.2−0.5 ppm. Given the enormous chemical shift changes observed when an acyl chain actually does bind an ACP (*11*), these minute perturbations were not significant and would probably not be detected even with a high-resolution structure of the acylated form. Nonetheless, we could not discount the possibility of small structural changes on the surface of the structure surrounding the phosphopantetheine group. We therefore recorded and analyzed a full complement of two- and three-dimensional NOESY spectra for the acylated form. ^{1}H assignments for the phosphopantetheine arm and the hexanoyl group were made from F_1- and F_2-filtered TOCSY and NOESY spectra, and analysis of the F_2-filtered two-dimensional NOESY and three-dimensional ^{13}C/^{15}N NOESY spectra revealed almost no differences from the holo form. The complete lack of NOEs from the acyl chain to the protein confirmed that NSAS ACP does not sequester the hexanoyl starter unit, and the lack of changes in the NOESY spectra suggests there is no change in the NSAS three-dimensional structure.

Structural Comparison with Other ACP Structures. A sequence-based multiple alignment against NSAS ACP revealed a lower degree of sequence similarity with other type I FAS/PKS ACPs (e.g., 20.5 and 28% similar in yeast and rat FAS and 32.2% in DEBS) than with type II FAS/PKS ACPs (43.2% in *E. coli* FAS and 42% in act PKS). Currently, there are only three type I ACP and two PCP domain structures available in the Protein Data Bank (PDB) for structural comparison. These are the FAS ACP domains from rat (*6*) and yeast (*27*), the ACP domain from module 2 of the 6-deoxyerythronolide B synthase (*7*), and the PCP/T domains from the tyrocidine (*23*, *28*) and the enterobactin nonribosomal peptide synthases (*29*). Structural alignment of NSAS ACP with these type I ACPs revealed that the degree of structural similarity was also low, although this improved significantly for the yeast and DEBS ACP when helix III was omitted from the comparison (Table 2). The alignment with rat FAS ACP remained poor. Comparison of NSAS ACP and the type II FAS ACPs, however, showed greater similarity in structure, with, again, the main difference being the orientation of helix III (Table 2 and Figure 5). The comparison with the type II PKS ACPs (act, otc, and fren) is also reasonable and is marginally better than that with the DEBS modular PKS ACP (cf. a rmsd over the backbone atoms of helices I, II, and IV of 2.49−2.61 Å vs 2.95 Å).

In the type II PKS/FAS ACPs, several conserved negatively charged residues in helix II function as a recognition site for synthase partners such as ACPS (*30*), FabH (*31*), FabG (*32*), MCAT (*33*), and $KS_\alpha KS_\beta$ (*34*). For example, a structure of the complex between ACP and ACPS from *B. subtilis* revealed that Glu41 and Asp48 formed salt bridges with positively charged residues on the surface of ACPS. A modeling and binding study of the ACP−FabH (ketosynthase III) complex from *E. coli* and the ACP−MCAT complex from *S. coelicolor* also showed that negatively charged residues in helix II of *E. coli* (Glu41, Glu47, Glu48, and Glu49) and *S. coelicolor* (Glu46, Glu52, and Glu53) ACPs were involved in complementary charge−charge interactions. However, the structure of the NSAS ACP reveals that the first of these is replaced with a hydrophobic residue, Val1751, while retaining a combination of positively and negatively charged residues (Arg1757, Glu1758, and Asp1759) at the C-terminal end. Figure 6 shows a comparison of 28 related nonreducing type I fungal PKS ACPs and confirms that the hydrophobicity at the position equivalent to Val1751 is

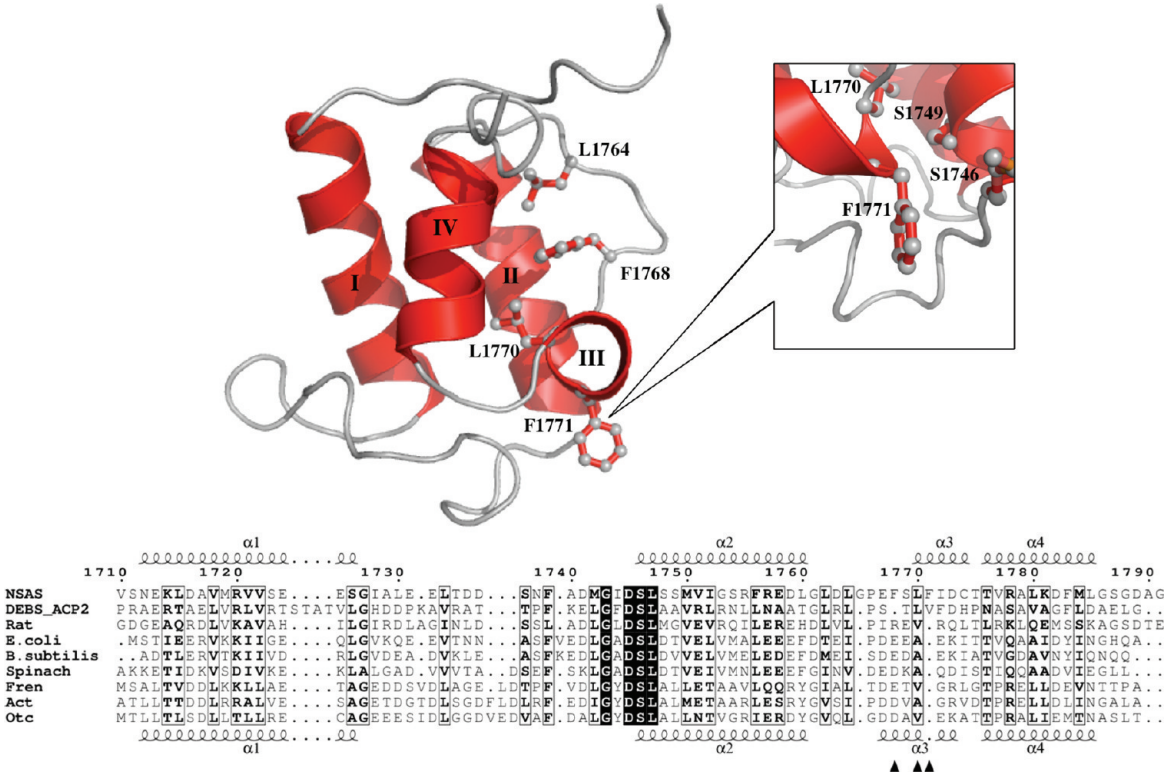

FIGURE 4: Structure of the NSAS ACP with an amino acid sequence alignment compared to other ACPs. The ACPs shown are from type I FAS (rat), type II FAS (*Escherichia coli*, *Bacillus subtilis*, and spinach), type I PKS (DEBS from module 2), and type II PKS (frenolicin, actinorhodin, and oxytetracycline). Secondary structures of NSAS ACP and type II FAS/PKS ACPs are shown at the top and bottom of the alignment, respectively. The residues restricting the motion of helix III of NSAS ACP are marked by black triangles.

Table 2: rmsd Values of the NSAS Holo ACP Structure Aligned with Various ACP Structures Using the McLachlan Algorithm (*45*) Implemented in Profit[a]

structural comparison of NSAS ACP with related ACP (PDB entry)	calculated rmsd value (Å)	
	overall (residues)	helices I, II, and IV (residues)
type I		
rat FAS (2PNG)	4.80 (3−77)	4.08 (3−16, 38−52, 66−74)
yeast FAS (2UV8)	6.31 (146−221)	3.90 (146−159, 181−194, 206−214)
DEBS PKS (2JU2)	7.88 (16−90)	2.95 (16−29, 55−69, 83−91)
type II		
Bs FAS (1HY8)	3.90 (2−76)	2.21 (2−15, 37−51, 65−73)
Mt FAS (1KLP)	3.80 (7−81)	2.56 (7−20, 41−55, 70−78)
Pf FAS (3GZM)	3.67 (5−79)	1.80 (5−18, 39−53, 68−76)
Sc FAS (2CNR)	3.56 (7−81)	2.22 (7−20, 41−55, 70−78)
Ec FAS (2K93)	3.52 (2−76)	2.20 (2−15, 36−50, 65−73)
act PKS (2K0X)	6.31 (5−79)	2.49 (5−18, 42−56, 71−79)
otc PKS (1NQ4)	6.39 (4−78)	2.61 (4−17, 41−55, 70−78)
fren PKS (1OR5)	4.34 (4−78)	2.50 (4−17, 40−54, 69−77)

[a]Ec, *E. coli*; Pf, *P. falciparum*; Bs, *B. subtilis*; Mt, *Mycobacterium tuberculosis*; Sc, *S. coelicolor*.

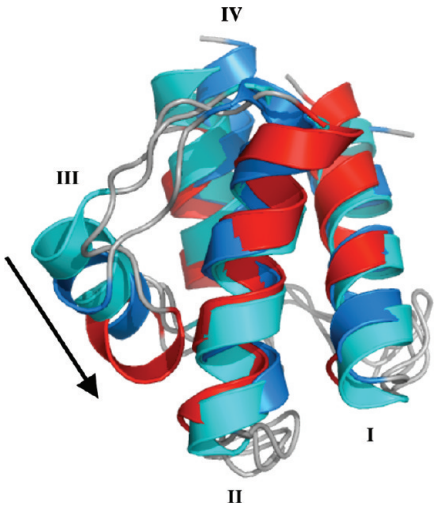

FIGURE 5: Superimposed structure of NSAS ACP (red) with *E. coli* (marine) and *Plasmodium falciparum* (cyan) type II FAS ACP showing the N-terminus of helix III of NSAS ACP is twisted down toward helix II.

well-conserved. Val1751 may be replaced with a polar or neutral residue in several of the ACPs, but there are no occurrences of charged residues. This position has been highlighted previously in the bacterial type I DEBS in which there are a total of six ACPs present (one per module). In this case, the presence of a positively or negatively charged residue at the position equivalent to Val1751 correlated with the ability for one ACP to substitute for another in the transfer of an intermediate to the KS domain in the next module (*35*). This residue is thought to control module to module selectivity. On the other hand, highly conserved charged residues on or around helix II of these ACPs, e.g., Asp53 of the DSL motif (equivalent to Asp1745) and Arg61 (equivalent to Gly1753), are thought to dictate conserved domain−domain interactions within a module (*7*). In the case of NSAS ACP, a hydrophobic or neutral amino acid may be important for domain−domain interactions specific to these synthases (e.g., interaction with SAT and PT domains). In the case of NSAS, this is not, however, over-riding as NSAS ACP interacts with $KS_{\alpha}KS_{\beta}$, albeit poorly (*15*).

Rigidity of Helix III in NSAS ACP May Prevent Starter Unit Binding. Type II FAS and PKS ACPs bind nonpolar

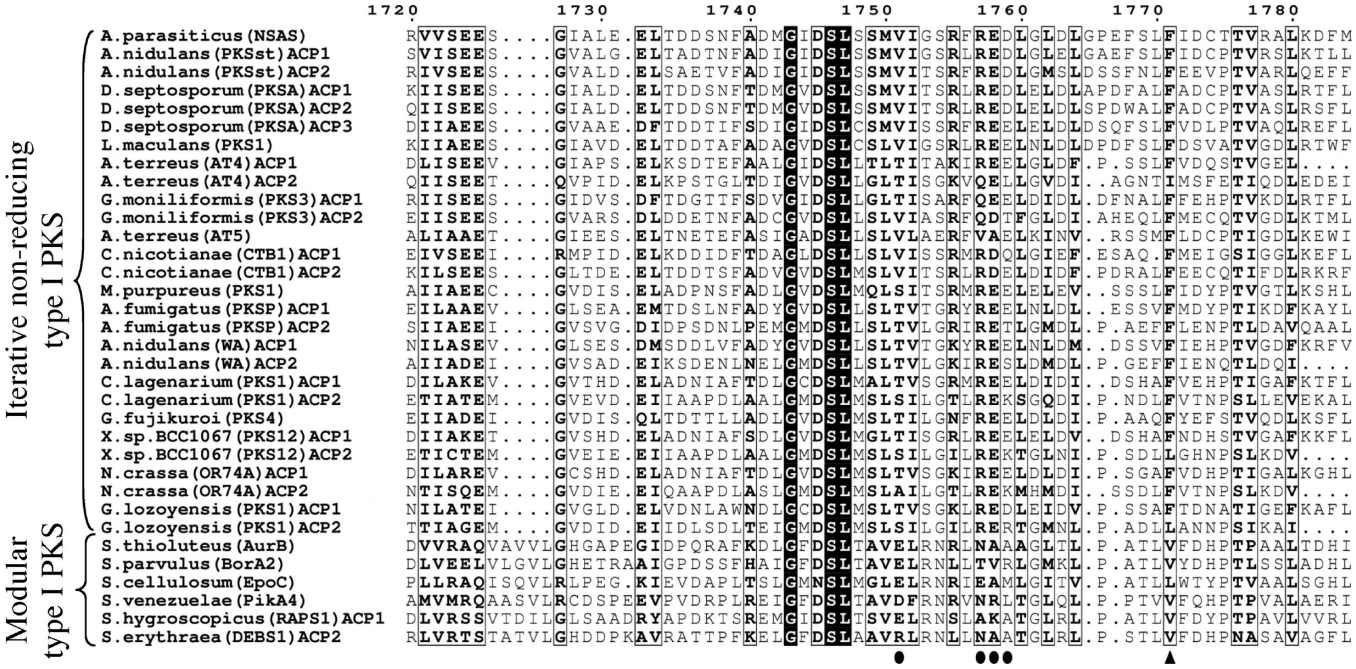

FIGURE 6: Sequence alignment of iterative nonreducing and modular type I PKS ACPs. The predicted recognition residues are marked with black circles, and the highly conserved Phe residue in iterative nonreducing type I ACPs is marked with a black triangle.

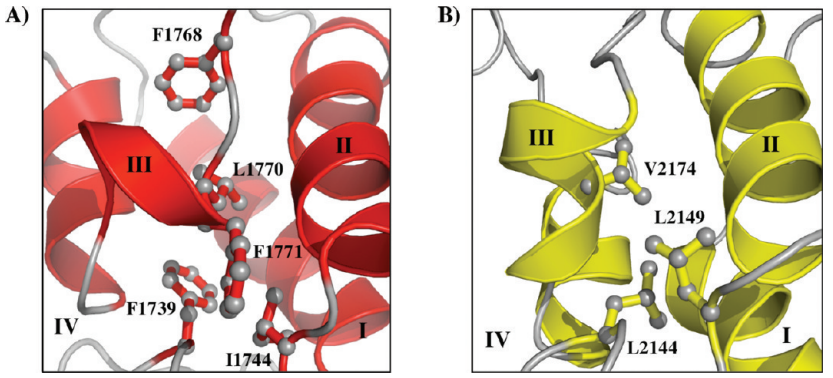

FIGURE 7: Structural comparison between (A) NSAS ACP (red) and (B) rat FAS ACP (yellow). The packing of residues from the loop underneath helices II and III and helix III illustrates the different ways in which binding of the acyl chain is prevented.

chains via internal binding cavities created in part by the movement of helix III away from helix II (*8*, *11*). In these ACPs, helix III is flexible and formed predominantly by charged residues. The consequent lack of hydrophobic packing within the protein may facilitate a transition to a more open form that allows insertion of the acyl chain. Figure 7A shows the helix II−helix III region of NSAS ACP. The side chain of Leu1770 points into the core of the structure with additional packing provided by Phe1768 and Phe1771. Therefore, unlike type II FAS/PKS ACPs, the formation of a stable hydrophobic core between these residues probably prevents helix III from moving to accommodate the hexanoyl moiety. This orientation of helix III is also similar to that of DEBS ACP2 in which residues Leu1770 and Phe1771 are replaced with Leu3389 and Val3390. These two residues are also highly conserved among modular type I PKSs (Figure 6). This suggests that helix III of DEBS ACP2 is inflexible and may also not bind acyl intermediates during biosynthesis, although this has not been tested to date. We have recently reported similar results for the rat type I FAS ACP for which we observed that hexanoyl and palmitoyl groups were not bound by the ACP (*6*). We also suggested that the analogous residues Leu2144 and Leu2149 from loop 1 and Val2174 from helix III form a well-packed stable triad that prevents the melting of helix III and the opening of a binding cavity (Figure 7B). The packing of the residues mentioned above is, however, arranged differently in NSAS ACP, and helix III of rat FAS ACP adopts a conformation more typical of other ACPs studied.

Sequence Comparison with Other Related Iterative Nonreducing Type I PKS ACPs. The sequence of NSAS ACP from *A. parasiticus* is highly similar (80%) with those of other iterative nonreducing type I PKS ACPs from synthases that produce similar toxins via a common NSA intermediate (Figure 6). For example, the sterigmatocystin PKS (PKS^{ST}) from *Aspergillus nidulans* (*36*) produces NSA; *Dothistroma septosporum* produces dothistromin which has a structure similar to that of the aflatoxin precursor versicolorin (*37*), and *Leptosphaeria maculans* also contains a PKS gene that is believed to be involved in aflatoxin biosynthesis (*38*). In contrast to NSAS, PKS^{ST} has a tandem ACP doublet also found in some other nonreducing fungal PKSs. Similarly, the dothistromin synthase from *Dothistroma septosporum* possesses a tandem ACP triplet, all of which are highly homologous to one another. Among all of these aflatoxin or aflatoxin-like producers, aromatic residues at positions equivalent to Phe1768 and Phe1771 are highly

conserved. This suggests that helix III of these ACP domains orients in the perpendicular position found in NSAS ACP and may be a common feature of iterative nonreducing type I PKS ACPs. This orientation of helix III may play a role alongside helix II in the domain−domain interactions specific to these synthases.

The remainder of the table alignment series in Figure 6 is comprised of ACPs selected from nonreducing fungal type I PKSs that produce other products such as tetrahydroxynaphthalene (THN). Included are PKSs from *Cercospora nicotianae* (*39*) and *Gibberella moniliformis* (*40*) (unidentified products) and the THN-producing PKSs from *Aspergillus fumigatus* (*41*) and *Collectotrichum lagenarium* (*42*). Like the type II ACPs, these sequences lack the insertion of several residues prior to helix III, and there is no conservation of Phe1768. However, unlike the type II ACPs, the hydrophobes at positions 1770 and 1771 are highly and completely conserved, respectively. Interestingly, in synthases in which there are two ACPs present, the bulky hydrophobe at position 1770 is always conserved in one of the pair, and this is usually the second ACP. The loop connecting helices II and III might therefore be correspondingly shorter, but a compensatory loss of the conserved aromatic residue equivalent to Phe1768 and conservation of these hydrophobes may indicate that helix III will again adopt a unique orientation in these ACPs. Future work to determine the high-resolution structure of this subclass of ACPs should reveal whether this feature is conserved.

It has been shown that the NSAS SAT domain displays a high selectivity for self-loading a hexanoyl group in marked preference to other chain lengths and subsequently transfers this to the ACP (*14*). The starter unit must then transfer to the KS to initiate polyketide biosynthesis followed by seven rounds of extension with malonyl-CoA extender units. By analogy to the porcine type I FAS structure, the resulting poly-β-keto chain may be protected by an internal chamber within the NSAS, where individual active sites may be accessed by the phosphopantetheine arm of the ACP and perhaps dynamic rearrangements of the synthase (*43*, *44*). The lack of ACP sequestration of the starter unit and possibly all later biosynthetic intermediates means the nascent polyketide may be passed efficiently back and forth between enzyme active sites. The ACP may play a passive role with respect to stabilization, whereas the adjacent PT domain has been shown to bind both linear and cyclized substrate mimics and may ultimately control the cyclization of the poly-β-keto chain. The lack of binding of a hydrophobic chain by NSAS ACP is consistent with our previous observation that the rat FAS type I ACP also exhibited no affinity for fatty acyl chains. There are currently no other examples of this behavior, but these results suggest that this is a distinct and important structural difference between type I and type II ACPs.

REFERENCES

1. Crump, M. P., Crosby, J., Dempsey, C. E., Parkinson, J. A., Murray, M., Hopwood, D. A., and Simpson, T. J. (1997) Solution structure of the actinorhodin polyketide synthase acyl carrier protein from *Streptomyces coelicolor* A3(2). *Biochemistry 36*, 6000–6008.
2. Li, Q., Khosla, C., Puglisi, J. D., and Liu, C. W. (2003) Solution structure and backbone dynamics of the holo form of the frenolicin acyl carrier protein. *Biochemistry 42*, 4648–4657.
3. Findlow, S. C., Winsor, C., Simpson, T. J., Crosby, J., and Crump, M. P. (2003) Solution structure and dynamics of oxytetracycline polyketide synthase acyl carrier protein from *Streptomyces rimosus*. *Biochemistry 42*, 8423–8433.
4. Zornetzer, G. A., Fox, B. G., and Markley, J. L. (2006) Solution structures of spinach acyl carrier protein with decanoate and stearate. *Biochemistry 45*, 5217–5227.
5. Sharma, A. K., Sharma, S. K., Surolia, A., Surolia, N., and Sarma, S. P. (2006) Solution structures of conformationally equilibrium forms of holo-acyl carrier protein (PfACP) from *Plasmodium falciparum* provides insight into the mechanism of activation of ACPs. *Biochemistry 45*, 6904–6916.
6. Płoskoń, E., Arthur, C. J., Evans, S. E., Williams, C., Crosby, J., Simpson, T. J., and Crump, M. P. (2008) A mammalian type I fatty acid synthase acyl carrier protein domain does not sequester acyl chains. *J. Biol. Chem. 283*, 518–528.
7. Alekseyev, V. Y., Liu, C. W., Cane, D. E., Puglisi, J. D., and Khosla, C. (2007) Solution structure and proposed domain domain recognition interface of an acyl carrier protein domain from a modular polyketide synthase. *Protein Sci. 16*, 2093–2107.
8. Upadhyay, S. K., Misra, A., Srivastava, R., Surolia, N., Surolia, A., and Sundd, M. (2009) Structural insights into the acyl intermediates of the *Plasmodium falciparum* fatty acid synthesis pathway: The mechanism of expansion of the acyl carrier protein core. *J. Biol. Chem. 284*, 22390–22400.
9. Roujeinikova, A., Baldock, C., Simon, W. J., Gilroy, J., Baker, P. J., Stuitje, A. R., Rice, D. W., Slabas, A. R., and Rafferty, J. B. (2002) X-ray crystallographic studies on butyryl-ACP reveal flexibility of the structure around a putative acyl chain binding site. *Structure 10*, 825–835.
10. Roujeinikova, A., Simon, W. J., Gilroy, J., Rice, D. W., Rafferty, J. B., and Slabas, A. R. (2007) Structural studies of fatty acyl-(acyl carrier protein) thioesters reveal a hydrophobic binding cavity that can expand to fit longer substrates. *J. Mol. Biol. 365*, 135–145.
11. Evans, S. E., Williams, C., Arthur, C. J., Płoskoń, E., Wattana-amorn, P., Cox, R. J., Crosby, J., Willis, C. L., Simpson, T. J., and Crump, M. P. (2009) Probing the interactions of early polyketide intermediates with the actinorhodin ACP from *Streptomyces coelicolor* A3(2). *J. Mol. Biol. 389*, 511–528.
12. Keatinge-Clay, A. T., Maltby, D. A., Medzihradszky, K. F., Khosla, C., and Stroud, R. M. (2004) An antibiotic factory caught in action. *Nat. Struct. Mol. Biol. 11*, 888–893.
13. Minto, R. E., and Townsend, C. A. (1997) Enzymology and molecular biology of aflatoxin biosynthesis. *Chem. Rev. 97*, 2537–2556.
14. Crawford, J. M., Dancy, B. C., Hill, E. A., Udwary, D. W., and Townsend, C. A. (2006) Identification of a starter unit acyl-carrier protein transacylase domain in an iterative type I polyketide synthase. *Proc. Natl. Acad. Sci. U.S.A. 103*, 16728–16733.
15. Ma, Y., Smith, L. H., Cox, R. J., Beltran-Alvarez, P., Arthur, C. J., and Simpson, T. J. (2006) Catalytic relationships between type I and type II iterative polyketide synthases: The *Aspergillus parasiticus* norsolorinic acid synthase. *ChemBioChem 7*, 1951–1958.
16. Crawford, J. M., Thomas, P. M., Scheerer, J. R., Vagstad, A. L., Kelleher, N. L., and Townsend, C. A. (2008) Deconstruction of iterative multidomain polyketide synthase function. *Science 320*, 243–246.
17. Cox, R. J., Crosby, J., Daltrop, O., Glod, F., Jarzabek, M. E., Nicholson, T. P., Reed, M., Simpson, T. J., Smith, L. H., Soulas, F., Szafranska, A. E., and Westcott, J. (2002) *Streptomyces coelicolor* phosphopantetheinyl transferase: A promiscuous activator of polyketide and fatty acid synthase acyl carrier proteins. *J. Chem. Soc., Perkin Trans. 1*, 1644–1649.
18. Delaglio, F., Grzesiek, S., Vuister, G. W., Zhu, G., Pfeifer, J., and Bax, A. (1995) NMRPipe: A multidimensional spectral processing system based on UNIX pipes. *J. Biomol. NMR 6*, 277–293.
19. Vranken, W. F., Boucher, W., Stevens, T. J., Fogh, R. H., Pajon, A., Llinas, M., Ulrich, E. L., Markley, J. L., Ionides, J., and Laue, E. D. (2005) The CCPN data model for NMR spectroscopy: Development of a software pipeline. *Proteins 59*, 687–696.
20. Delaglio, F., Cornilescu, G., and Bax, A. (1999) Protein backbone angle restraints from searching a database for chemical shift and sequence homology. *J. Biomol. NMR 13*, 289–302.
21. Linge, J. P., O'Donoghue, S. I., and Nilges, M. (2001) Automated assignment of ambiguous nuclear Overhauser effects with ARIA. *Methods Enzymol. 339*, 71–90.
22. Nederveen, A. J., Doreleijers, J. F., Vranken, W., Miller, Z., Spronk, C. A., Nabuurs, S. B., Güntert, P., Livny, M., Markley, J. L., Nilges, M., Ulrich, E. L., Kaptein, R., and Bonvin, A. M. (2005) RECOORD: A recalculated coordinate database of 500+ proteins from the PDB using restraints from the BioMagResBank. *Proteins 59*, 662–672.
23. Koglin, A., Mofid, M. R., Löhr, F., Schafer, B., Rogov, V. V., Blum, M. M., Mittag, T., Marahiel, M. A., Bernhard, F., and Dotsch, V. (2006) Conformational switches modulate protein interactions in peptide antibiotic synthetases. *Science 312*, 273–276.
24. Hooft, R. W., Vriend, G., Sander, C., and Abola, E. E. (1996) Errors in protein structures. *Nature 381*, 272.

25. Laskowski, R. A., Rullmannn, J. A., MacArthur, M. W., Kaptein, R., and Thornton, J. M. (1996) AQUA and PROCHECK-NMR: Programs for checking the quality of protein structures solved by NMR. *J. Biomol. NMR 8*, 477–486.
26. Evans, S. E., Williams, C., Arthur, C. J., Burston, S. G., Simpson, T. J., Crosby, J., and Crump, M. P. (2008) An ACP structural switch: Conformational differences between the apo and holo forms of the actinorhodin polyketide synthase acyl carrier protein. *ChemBioChem 9*, 2424–2432.
27. Leibundgut, M., Jenni, S., Frick, C., and Ban, N. (2007) Structural basis for substrate delivery by acyl carrier protein in the yeast fatty acid synthase. *Science 316*, 288–290.
28. Weber, T., Baumgartner, R., Renner, C., Marahiel, M. A., and Holak, T. A. (2000) Solution structure of PCP, a prototype for the peptidyl carrier domains of modular peptide synthetases. *Structure 8*, 407–418.
29. Frueh, D. P., Arthanari, H., Koglin, A., Vosburg, D. A., Bennett, A. E., Walsh, C. T., and Wagner, G. (2008) Dynamic thiolation-thioesterase structure of a non-ribosomal peptide synthetase. *Nature 454*, 903–906.
30. Parris, K. D., Lin, L., Tam, A., Mathew, R., Hixon, J., Stahl, M., Fritz, C. C., Seehra, J., and Somers, W. S. (2000) Crystal structures of substrate binding to *Bacillus subtilis* holo-(acyl carrier protein) synthase reveal a novel trimeric arrangement of molecules resulting in three active sites. *Structure 8*, 883–895.
31. Zhang, Y. M., Rao, M. S., Heath, R. J., Price, A. C., Olson, A. J., Rock, C. O., and White, S. W. (2001) Identification and analysis of the acyl carrier protein (ACP) docking site on β-ketoacyl-ACP synthase III. *J. Biol. Chem. 276*, 8231–8238.
32. Zhang, Y. M., Wu, B., Zheng, J., and Rock, C. O. (2003) Key residues responsible for acyl carrier protein and β-ketoacyl-acyl carrier protein reductase (FabG) interaction. *J. Biol. Chem. 278*, 52935–52943.
33. Arthur, C. J., Williams, C., Pottage, K., Płoskoń, E., Findlow, S. C., Burston, S. G., Simpson, T. J., Crump, M. P., and Crosby, J. (2009) Structure and malonyl CoA-ACP transacylase binding of *Streptomyces coelicolor* fatty acid synthase acyl carrier protein. *ACS Chem. Biol. 4*, 625–636.
34. Beltran-Alvarez, P., Arthur, C. J., Cox, R. J., Crosby, J., Crump, M. P., and Simpson, T. J. (2009) Preliminary kinetic analysis of acyl carrier protein-ketoacylsynthase interactions in the actinorhodin minimal polyketide synthase. *Mol. Biosyst. 5*, 511–518.
35. Wu, N., Cane, D. E., and Khosla, C. (2002) Quantitative analysis of the relative contributions of donor acyl carrier proteins, acceptor ketosynthases, and linker regions to intermodular transfer of intermediates in hybrid polyketide synthases. *Biochemistry 41*, 5056–5066.
36. Yu, J. H., and Leonard, T. J. (1995) Sterigmatocystin biosynthesis in *Aspergillus nidulans* requires a novel type I polyketide synthase. *J. Bacteriol. 177*, 4792–4800.
37. Zhang, S., Schwelm, A., Jin, H., Collins, L. J., and Bradshaw, R. E. (2007) A fragmented aflatoxin-like gene cluster in the forest pathogen *Dothistroma septosporum*. *Fungal Genet. Biol. 44*, 1342–1354.
38. Gardiner, D. M., Cozijnsen, A. J., Wilson, L. M., Pedras, M. S., and Howlett, B. J. (2004) The sirodesmin biosynthetic gene cluster of the plant pathogenic fungus *Leptosphaeria maculans*. *Mol. Microbiol. 53*, 1307–1318.
39. Choquer, M., Dekkers, K. L., Chen, H. Q., Cao, L., Ueng, P. P., Daub, M. E., and Chung, K. R. (2005) The CTB1 gene encoding a fungal polyketide synthase is required for cercosporin biosynthesis and fungal virulence of *Cercospora nicotianae*. *Mol. Plant-Microbe Interact. 18*, 468–476.
40. Kroken, S., Glass, N. L., Taylor, J. W., Yoder, O. C., and Turgeon, B. G. (2003) Phylogenomic analysis of type I polyketide synthase genes in pathogenic and saprobic ascomycetes. *Proc. Natl. Acad. Sci. U.S.A. 100*, 15670–15675.
41. Langfelder, K., Jahn, B., Gehringer, H., Schmidt, A., Wanner, G., and Brakhage, A. A. (1998) Identification of a polyketide synthase gene (*pks*P) of *Aspergillus fumigatus* involved in conidial pigment biosynthesis and virulence. *Med. Microbiol. Immunol. 187*, 79–89.
42. Takano, Y., Kubo, Y., Shimizu, K., Mise, K., Okuno, T., and Furusawa, I. (1995) Structural analysis of PKS1, a polyketide synthase gene involved in melanin biosynthesis in *Colletotrichum lagenarium*. *Mol. Gen. Genet. 249*, 162–167.
43. Crawford, J. M., Korman, T. P., Labonte, J. W., Vagstad, A. L., Hill, E. A., Kamari-Bidkorpeh, O., Tsai, S., and Townsend, C. A. (2009) Structural basis for biosynthetic programming of fungal aromatic polyketide cyclization. *Nature 461*, 1139–1144.
44. Maier, T., Jenni, S., and Ban, N. (2006) Architecture of mammalian fatty acid synthase at 4.5 Å resolution. *Science 311*, 1258–1262.
45. Mclachlan, A. D. (1982) Rapid comparison of protein structures. *Acta Crystallogr. A38*, 871–873.